Observation of α decay from a state in ^{10}B at 11.48 MeV

O. S. Kirsebom,[1,*] M. Alcorta,[2,†] M. J. G. Borge,[2] M. Cubero,[2] H. O. U. Fynbo,[1] M. Madurga,[2,‡] and O. Tengblad[2]

[1]*Department of Physics and Astronomy, Aarhus University, DK-8000 Aarhus C, Denmark*

[2]*Instituto de Estructura de la Materia, CSIC, Serrano 113 bis, E-28006 Madrid, Spain*

(Received 13 December 2011; published 9 May 2012)

We report on the observation of α decay from a state in ^{10}B at 11.48 MeV. The only observed decay branch is to the first $T = 1$ state in ^{6}Li at 3.56 MeV. The apparent absence of an α-decay branch to the ($T = 0$) ground state in ^{6}Li suggests that the 11.48-MeV state should be assigned isospin $T = 1$. The spin and parity of the 11.48-MeV state could not be directly determined from the present study apart from $J = 0$ being ruled out by the observed angular correlation. We conjecture that the 11.48-MeV state is the analog of the 10.15-MeV, (4^+) state in ^{10}Be, constitutes the third member of a rotational band built on the 0^+ state at 7.65 MeV, and has pronounced molecular structure.

DOI: 10.1103/PhysRevC.85.054308 PACS number(s): 21.10.Gv, 21.10.Re, 25.55.−e, 27.20.+n

I. INTRODUCTION

The concept of nuclear molecules, i.e., nuclei composed of inert clusters and additional valence nucleons, is nearly as old as the field of nuclear physics itself [1]. Well-known examples of nuclei exhibiting molecular structure are ^{9,10}Be and ^{13,14}C where α particles play the role of inert clusters and neutrons play the role of valence nucleons [2].

As outlined in Ref. [3], experimental efforts during the past 10–15 years have established the existence of a rotational band built on the second 0^+ state in ^{10}Be at 6.18 MeV. The second and third members of the band, the 2^+ and 4^+ excitations, are located at 7.54 and 10.15 MeV, respectively. The moment of inertia deduced from the energy separation of the band members is roughly 2.5 times larger than the moment of inertia of the ^{8,9,10}Be ground-state bands, indicating pronounced molecular structure and a greatly enhanced separation of the two α clusters. We note that the spin-parity of the 10.15-MeV state remains somewhat controversial. It was first found to be 3^- [4,5], but two more recent measurements [6,7] both favor a 4^+ assignment.

Related to this is the unusually large α width of the 7.54-MeV state [6,8], which exceeds the Wigner limit [9] by a factor of $\sim$50.[1] The enhanced separation of the two α clusters may partially explain the large α width since it results in a lowering of the centrifugal and Coulomb barriers, which inhibit the decay very strongly because the 7.54-MeV state is located only 129 keV above the $\alpha + {}^6$He threshold; see, e.g., the analysis of Ref. [3]. Nevertheless, a new measurement of the α width of the 7.54-MeV state is desirable. The analog 2^+ state in ^{10}B also has a very large α width [10], but in this case there is nothing unusual about the width, which is comparable to the Wigner limit.

Given the unusual character of the rotational band built on the 6.18-MeV state in ^{10}Be, it is of considerable interest to identify the analog $T = 1$ states in ^{10}B and ^{10}C. In ^{10}B, the analogs of the 6.18- and 7.54-MeV states are located at 7.56 and 8.89 MeV while the analog of the 10.15-MeV state has not yet been identified experimentally. Theoretically, it is expected to be around 11.6 MeV [3].

As noted in Ref. [11], the 10.15-MeV state in ^{10}Be exhibits peculiar decay properties. While particle unbound states in ^{10}Be usually decay by neutron emission, the 10.15-MeV state has only been observed to decay by α emission [6,7,12,13]. It has a very large α width comparable to the Wigner limit [7], and it decays both to the 0^+ ground state and the 2^+ first-excited state in ^{6}He [13]. One may reasonably assume similar decay properties for the analog state in ^{10}B, i.e., the decay should be dominated by α emission to the 0^+ and 2^+, $T = 1$ states in ^{6}Li located at 3.56 and 5.37 MeV, respectively. Indeed, a recent conference proceedings paper [14] reports a state at $\sim$11.3 MeV, populated in the reaction $^{3}\mathrm{He} + {}^{11}\mathrm{B} \rightarrow \alpha + {}^{10}\mathrm{B}$, that decays by α emission to the 3.56-MeV state in ^{6}Li.

In the present paper, we present results from a measurement of the $^{3}\mathrm{He} + {}^{11}\mathrm{B}$ reaction carried out in 2008. We find firm experimental evidence for the existence of a state in ^{10}B at 11.48 MeV that decays by α emission to the 3.56-MeV state in ^{6}Li as illustrated in Fig. 1. We thus confirm the observation of Ref. [14], but with higher statistics and improved resolution. We conjecture that the 11.48-MeV state is the analog of the 10.15-MeV, (4^+) state in ^{10}Be and constitutes the third member of a rotational band built on the 0^+ state at 7.65 MeV.

II. EXPERIMENT

The experiment was carried out at the Centro de Microanálisis de Materiales in Madrid. A 5-MV tandem accelerator was used to accelerate the ^{3}He beam to 8.5 MeV. The target consisted of 22 μg/cm^2 natural boron evaporated on a 4 μg/cm^2 carbon support foil. The detection system consisted of four ΔE-E telescopes, each consisting of a 60-μm-thick double-sided silicon strip detector (DSSSD) backed by a 1.5-mm-thick unsegmented silicon detector. The

*Corresponding author: oliskir@phys.au.dk; Present address: TRIUMF, Vancouver, BC V6T 2A3, Canada.

†Present address: Physics Division, Argonne National Laboratory, Argonne, IL 60439, USA.

‡Present address: Department of Physics and Astronomy, University of Tennessee, Knoxville, TN 37996, USA.

[1]This result is obtained by assuming a standard channel radius of 4.8 fm = 1.4 fm $\times$ ($4^{1/3} + 6^{1/3}$); if a channel radius of 6.2 fm is used, the factor is $\sim$10.

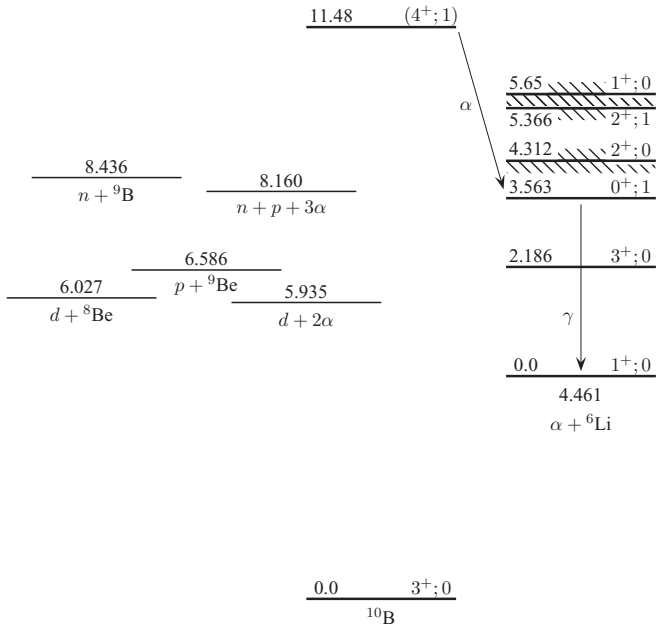

FIG. 1. Decay scheme showing the decay branch observed in the present experiment. States are labeled by their excitation energy in MeV, spin-parity, and isospin. In ^{10}B, only the ground state and the 11.48-MeV state are shown. In ^{6}Li all known [15] energetically accessible states are shown. Threshold energies are from Ref. [16].

intrinsic resolution, given as the full width at half maximum, of the DSSSDs was 35 keV while that of the E detectors was 40–50 keV. The detectors were placed 4 cm from the target with two of them covering 7°–75° relative to the beam axis and the other two covering 98°–170°, resulting in a total solid-angle coverage of 38% of 4π. One DSSSD had 32×32 strips of 2 mm width, and the other three 16×16 strips of 3 mm width, resulting in an angular resolution of 2° and 3°, respectively.

The strength of the setup lies in its ability to provide complete kinematical information for reaction channels leading to many-body final states. The efficiencies for detecting triple and quadruple coincidences are on the order of 5% and 1%, respectively. See Refs. [17,18] for details. We note that the detectors are insensitive to γ rays and neutrons; only charged particles are measured, but γ-ray and neutron energies can still be determined indirectly by use of energy and momentum conservation [19].

III. DATA ANALYSIS

A. General remarks

The ^{3}He + ^{11}B reaction at 8.5 MeV leads to a multitude of many-body final states, in most cases with several contributing channels. An exhaustive analysis is beyond the scope of the present paper, and we limit ourselves to the reaction channels of direct relevance.

At a beam energy of 8.5 MeV, states up to 15.80 MeV can be populated in the ^{3}He + ^{11}B → α + ^{10}B reaction (Q = 9.12 MeV). Depending on the excitation energy, the following decay modes are possible: γ, n, p, d, α (see Fig. 1). We note that neutron decay (n) invariably leads to the five-body final state $n + p + 3\alpha$ because ^{9}B and ^{8}Be are unbound, whereas proton decay (p) also can lead to the three-body final state $p + \alpha + {}^{9}$Be if the decay proceeds to the ground state in ^{9}Be. Deuteron decay (d) invariably leads to the four-body final state $d + 3\alpha$. Finally, α decay can lead to $n + p + 3\alpha$ and $d + 3\alpha$ if the decay proceeds to unbound states in ^{6}Li, but it can also lead to the three-body final state $2\alpha + {}^{6}$Li if the decay proceeds to the ground state in ^{6}Li or to an excited state with a significant γ branch, which, according to Ref. [16], is the case only for the 3.56-MeV state.

In the present experiment, we identify states in ^{10}B decaying by γ, p, d, and α emission, but we find no clear evidence for states decaying by neutron emission. (Our failure to observe neutron decay is probably due to a combination of two factors: a reduced detection efficiency owing to the high multiplicity of the $n + p + 3\alpha$ final state and the presence of many competing channels, some involving very broad intermediate states.) The results are generally consistent with the TUNL evaluation [16] and are summarized in Table I. The main new result is the observation of the α decay of a state at 11.48 MeV. Weak evidence for this decay was previously reported in Ref. [14]. Below we describe the kinematical cuts used to identify the decay in the present experiment.

B. Event selection

The kinematics of the ^{3}He + ^{11}B → 2α + ^{6}Li reaction is such that at most one α particle has enough energy to penetrate into the E detector, while the ^{6}Li ion and at least one α particle always are stopped in the ΔE detector, preventing particle identification via the ΔE-E method. To distinguish the triple coincidences owing to $2\alpha + {}^{6}$Li from the vast background of other triple coincidences, we rely on energy and momentum conservation: Each triple coincidence detected is assumed to consist of two α particles and a ^{6}Li ion (unless, of course, the ΔE-E method has positively identified one of the particles as being something else). The momentum of each particle is calculated as $\vec{p}_i = (2m_i E_i)^{1/2}\hat{n}_i$, where E_i is the measured energy, $\hat{n}_i$ is direction of emission, and m_i is the assumed mass. The momentum deficit, $\delta P = |\sum_i \vec{p}_i - \vec{p}_0|$, where $\vec{p}_0$ denotes the beam momentum, is calculated for the three possible choices of which detected particle is the ^{6}Li ion. The choice producing the smallest value of δP is selected. The energy deficit is calculated as $\delta E = \sum_i E_i + Q - E_0$, where Q = 4.66 MeV is the Q value of the ^{3}He + ^{11}B → 2α + ^{6}Li reaction and E_0 = 8.5 MeV is the beam energy. Finally, we plot δP against δE to obtain Fig. 2. The loci corresponding to $2\alpha + {}^{6}$Li(gs) and $2\alpha + {}^{6}$Li(3.56) are indicated by red circles. In the latter case, the missing energy has been carried away by a γ ray with negligible momentum. Similar kinematical cuts may be applied to select other event types such as $p + \alpha + {}^{9}$Be, $d + 3\alpha$, and $n + p + 3\alpha$.

C. Excitation spectra

Having selected the events of interest, we wish to construct a ^{10}B excitation spectrum. *A priori*, we cannot say which, if any, is the primary α particle, emitted in the first step of the reaction, ^{3}He + ^{11}B → α + ^{10}B, and which is the secondary

TABLE I. Peaks seen in the various decay spectra. Each peak is identified with one or several known [16] states in ^{10}B.

Present study		TUNL [16]			
Decay	E_x (MeV $\pm$ keV)	E_x (MeV $\pm$ keV)	$J^\pi; T$	Γ (keV)	Decay
	0.003 $\pm$ 3[a]	gs	$3^+; 0$	stable	
	0.717 $\pm$ 4	0.71835 $\pm$ 0.04	$1^+; 0$	$\tau_m = 1.020 \pm 0.005$ ns	γ
$\gamma + {}^{10}$B	1.736 $\pm$ 6	1.74015 $\pm$ 0.17	$0^+; 1$	7 $\pm$ 3 fs	γ
	2.157 $\pm$ 4	2.1543 $\pm$ 0.5	$1^+; 0$	2.13 $\pm$ 0.20 ps	γ
	3.587 $\pm$ 6	3.5871 $\pm$ 0.5	$2^+; 0$	153 $\pm$ 12 fs	γ
	5.165 $\pm$ 2	5.1639 $\pm$ 0.6	$2^+; 1$	1.8 $\pm$ 0.4 eV	γ, α
	6.995 $\pm$ 11	7.002 $\pm$ 6	$(3^+); 0$	100 $\pm$ 10	p, d, α
	8.762 $\pm$ 14	8.68[b]	$(3^+); 0$		p
$d + {}^8$Be(gs)		8.889 $\pm$ 6	$3^-; 1$	84 $\pm$ 7	n, p, α
		8.894 $\pm$ 2	$2^+; 1$	40 $\pm$ 1	p, α
	6.936 $\pm$ 30	6.873 $\pm$ 5	$1^-; 0+1$	120 $\pm$ 5	γ, p, d, α
$d + {}^8$Be(2^+)		7.002 $\pm$ 6	$(3^+); 0$	100 $\pm$ 10	p, d, α
	7.573 $\pm$ 14	(7.67 $\pm$ 30)	$(1^+; 0)$	250 $\pm$ 20	$p, (d), \alpha$
	7.515 $\pm$ 22	7.469 $\pm$ 6	$2^+; 1$	65 $\pm$ 10	γ, p
		7.480 $\pm$ 4	$2^-; 0+1$	80 $\pm$ 8	γ, p, d, α
		7.5599 $\pm$ 0.6	$0^+; 1$	2.65 $\pm$ 0.18	γ, p
$p + {}^9$Be(gs)	8.893 $\pm$ 11	8.889 $\pm$ 6	$3^-; 1$	84 $\pm$ 7	n, p, α
		8.894 $\pm$ 2	$2^+; 1$	40 $\pm$ 1	p, α
	10.931 $\pm$ 20	10.83 $\pm$ 10	$(2^+, 3^+, 4^+)$	300 $\pm$ 100	γ, n, p
	12.533 $\pm$ 11	12.56 $\pm$ 30		100 $\pm$ 30	γ, p
	4.779 $\pm$ 11	4.7740 $\pm$ 0.5	$3^+; 0$	7.8 $\pm$ 1.2 eV	γ, α
	5.144 $\pm$ 12	5.1639 $\pm$ 0.6	$2^+; 1$	1.8 $\pm$ 0.4 eV	γ, α
		5.180 $\pm$ 10	$1^+; 0$	110 $\pm$ 10	γ, α
$\alpha + {}^6$Li(gs)	6.038 $\pm$ 20	6.0250 $\pm$ 0.6	$4^+; 0$	0.054 $\pm$ 0.024	γ, α
		6.1272 $\pm$ 0.7	$3^-; 0$	1.52 $\pm$ 0.08	α
	6.549 $\pm$ 11	6.560 $\pm$ 1.9	$4^-; 0$	25.1 $\pm$ 1.1	α
	7.000 $\pm$ 12	7.002 $\pm$ 6	$(3^+); 0$	100 $\pm$ 10	p, d, α
$\alpha + {}^6$Li(3^+)	7.414 $\pm$ 14	7.96 $\pm$ 70[c]	$T = 0$	285 $\pm$ 91	$\alpha, {}^6$Li(3^+)
	9.719 $\pm$ 30	9.58 $\pm$ 60[c]	$T = 0$	257 $\pm$ 64	$\alpha, {}^6$Li(3^+)
	8.887 $\pm$ 10	8.889 $\pm$ 6	$3^-; 1$	84 $\pm$ 7	n, p, α
$\alpha + {}^6$Li(3.56)		8.894 $\pm$ 2	$2^+; 1$	40 $\pm$ 1	p, α
	11.483 $\pm$ 27	11.52 $\pm$ 35		500 $\pm$ 100	$(\gamma), \alpha$

[a]The γ-decay spectrum was recalibrated using the evaluated energies in the third column.
[b]The width is presumably $\Gamma \approx 220$ keV and decay modes of d and α are likely [16].
[c]The energies fit poorly; the identification is mainly based on the observed decay to ^{6}Li(3^+).

α particle, resulting from the subsequent decay of ^{10}B. We deal with this ambiguity by exploring both possibilities: We calculate the excitation energy corresponding to one sequence of emission, ε_{ij}, and that corresponding to the opposite sequence of emission, ε_{ji}, and plot the two against each other as done in Figs. 3(a) and 4(a). States in ^{10}B are seen as horizontal and vertical bands. Diagonal bands corresponding to the channels ^{6}Li + ^{8}Be(gs) and ^{6}Li + ^{8}Be(2^+) are also seen (but in this case, the question of the ordering of the α particles clearly has no meaning). In both figures the horizontal, vertical, and diagonal bands account for ~90% of the observed events.

Five horizontal-vertical bands are visible in Fig. 3(a), which shows the $2\alpha + {}^6$Li(gs) events. Corresponding peaks are visible in Fig. 3(b) and have been labeled $\alpha 1$–$\alpha 5$. We identify $\alpha 1$ with the 3^+, $T = 0$ state at 4.77 MeV, $\alpha 2$ with the 2^-, $T = 0$ state at 5.11 MeV and the 2^+, $T = 1$ state at 5.16 MeV, unresolved owing to the finite experimental resolution, $\alpha 3$ with the 4^+, $T = 0$ state at 6.03 MeV and the 3^-, $T = 0$ state at 6.13 MeV, again, unresolved owing to the finite experimental resolution, $\alpha 4$ with the 4^-, $T = 0$ state at 6.56 MeV, and $\alpha 5$ with the (3^+), $T = 0$ state at 7.00 MeV.

Three horizontal-vertical bands are visible in Fig. 4(a), which shows the $2\alpha + {}^6$Li(3.56) events. Corresponding peaks are visible in Fig. 4(b) and have been labeled $\alpha 6$–$\alpha 8$. We are unable to identify $\alpha 6$, which is centered at 8.27 MeV, with any known state in ^{10}B. In fact, we believe $\alpha 6$ to be an experimental artifact caused by a sharp increase in the triple-coincidence detection efficiency close to the $\alpha + {}^6$Li(3.56) threshold, where the relative energy of the decay fragments becomes low

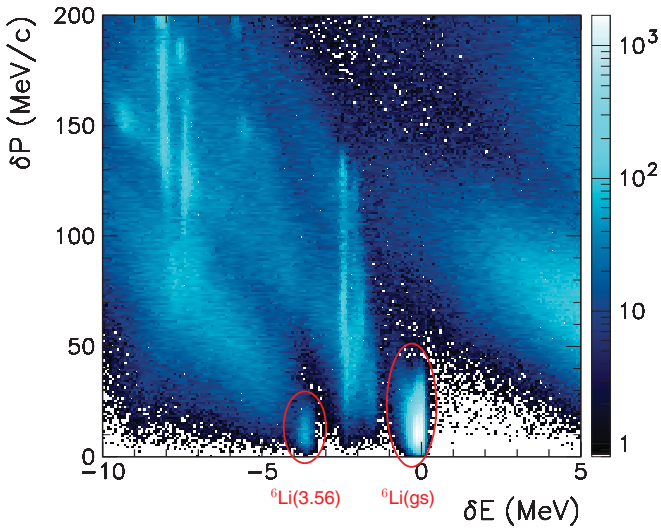

FIG. 2. (Color online) Kinematical cuts used for event selection; δE and δP are the energy and momentum deficits (see text). Loci corresponding to $2\alpha + {}^6$Li(gs) and $2\alpha + {}^6$Li(3.56) are indicated by red circles.

enough for both of them to hit the same detector irrespective of the orientation of the decay. Indeed, using a Monte Carlo simulation program validated in several previous studies [17,19,21], we find that the average detection efficiency below 8.8 MeV is

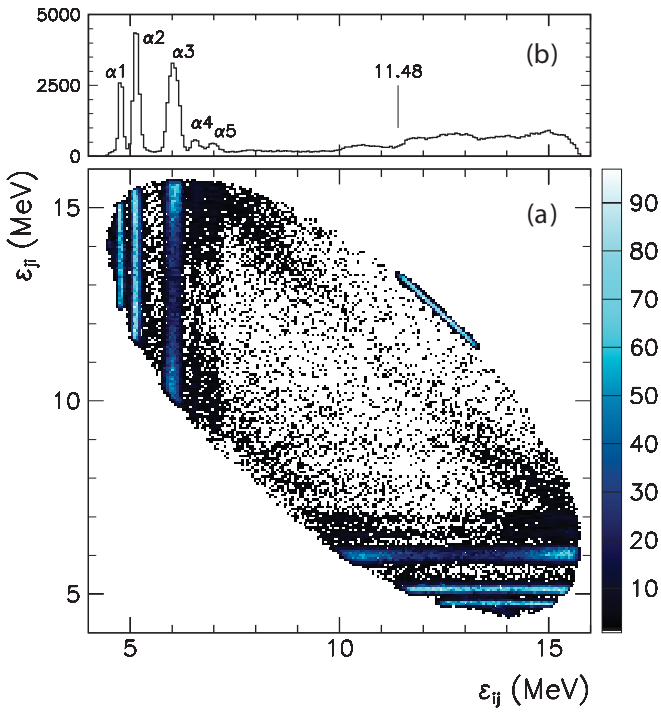

FIG. 3. (Color online) (a) Two-dimensional excitation spectrum showing $2\alpha + {}^6$Li(gs) events; ε_{ij} and ε_{ji} are the ^{10}B excitation energies calculated by assuming opposite orderings of the α particles. States in ^{10}B are seen as horizontal and vertical bands. Diagonal bands corresponding to the channels ^{6}Li(gs) + ^{8}Be(gs) and ^{6}Li(gs) + ^{8}Be(2^+) are also visible. (b) Projection on the abscissa. The position where the 11.48-MeV peak would have been visible is indicated.

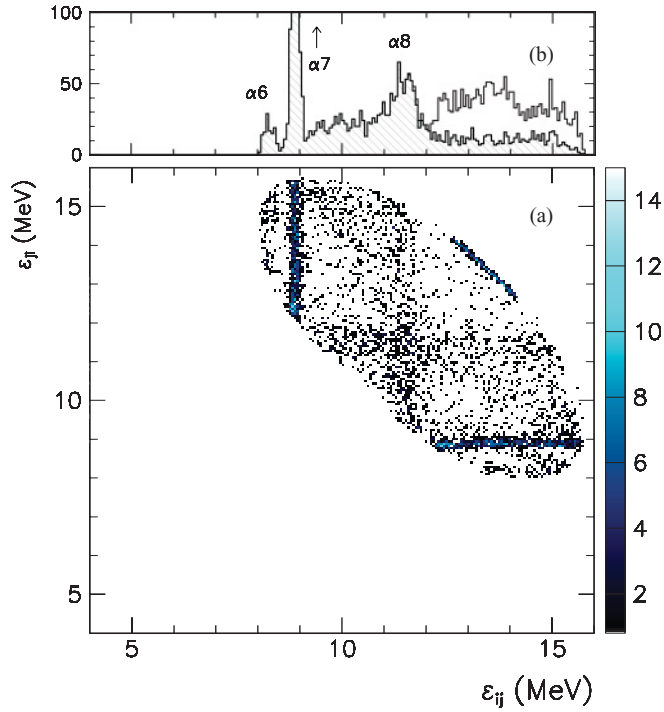

FIG. 4. (Color online) (a) Two-dimensional excitation spectrum showing $2\alpha + {}^6$Li(3.56) events; ε_{ij} and ε_{ji} are the ^{10}B excitation energies calculated by assuming opposite orderings of the α particles. States in ^{10}B are seen as horizontal and vertical bands. Diagonal bands corresponding to the channels ^{6}Li(3.56) + ^{8}Be(gs) and ^{6}Li(3.56) + ^{8}Be(2^+) are also visible. (b) Projection on the abscissa. The background above the 11.48-MeV state can be reduced (hatched histogram) by placing an antigate on ^{8}Be(gs) and requiring $\varepsilon_{ji} > 9.4$ MeV.

about a factor of 20 higher than above 8.8 MeV. We identify $\alpha 7$ with the closely spaced 3^- and 2^+, $T = 1$ states at 8.89 MeV, unresolved owing to the finite experimental resolution, and $\alpha 8$ with a state at 11.52(4) MeV of unknown spin, parity, and isospin but seen in several previous experiments [16] including a previous measurement of the ^{3}He + ^{11}B $\rightarrow \alpha + {}^{10}$B reaction [20]. This state is the subject of the present paper, and we determine the energy to be 11.48(3) MeV.

IV. RESULTS AND DISCUSSION

In this section we present results concerning the closely spaced 3^- and 2^+, $T = 1$ states at 8.89 MeV, henceforth referred to as the $2^+/3^-$ doublet, and the 11.48-MeV state. We use $\Gamma_{\alpha(\mathrm{gs})}$ to denote the partial width for α decay to ^{6}Li(gs) and $\Gamma_{\alpha(3.56)}$ to denote the partial width for α decay to ^{6}Li(3.56). Monte Carlo simulations were used to determine the relative detection efficiencies of the various decay channels. Angular distributions were assumed to be isotropic. This simplifying assumption causes a systematic uncertainty in the determination of the relative detection efficiencies, which has been estimated to be ∼20%.

A. The $2^+/3^-$ doublet at 8.89 MeV

The two states are very close in energy (~5 keV separation) and have similar widths (both below the experimental resolution), so we are unable to separate them experimentally. The doublet is seen both in the $p + {}^9$Be decay spectrum and the $\alpha + {}^6$Li(3.56) decay spectrum. We are able to determine the ratio of proton decays to α decays for the doublet as a whole. Corrected for detection efficiencies, the ratio is 1.0(2). Unfortunately, we are unable to determine the ratio for the states separately because we do not know the relative feeding of the states. According to Ref. [10] the ratio is $\Gamma_p/\Gamma_{\alpha(3.56)} = 0.39(10)$ for the 2^+ state and $\Gamma_p/\Gamma_{\alpha(3.56)} = 132(21)$ for the 3^- state. Using these numbers and the ratio of 1.0(2) obtained for the doublet as a whole, we infer a relative feeding of $2^+/3^- = 2.2(4)$ and conclude that the 3^- state contributes less than 1% to the peak in the $\alpha + {}^6$Li(3.56) decay spectrum.

No peak is seen at 8.89 MeV in the $\alpha + {}^6$Li(gs) decay spectrum. This allows us to place an upper limit on the ratio $\Gamma_{\alpha(\mathrm{gs})}/\Gamma_{\alpha(3.56)}$ for the 2^+ state. Corrected for detection efficiencies, the upper limit is

$$\frac{\Gamma_{\alpha(\mathrm{gs})}}{\Gamma_{\alpha(3.56)}} < 0.04$$

at 95% C.L.

Owing to the smaller difference in energy between the initial and final state, the decay to the 3.56-MeV state is more strongly inhibited by the centrifugal and Coulomb barrier than the decay to the ground state. The reduced width, γ^2, is often introduced as a measure of what may be considered the intrinsic (nuclear) decay width. It is related to the observed decay width as $\Gamma = 2P_\ell(E)\gamma^2$, where E is the relative kinetic energy of the decay products and $P_\ell(E)$ is the probability of penetrating the centrifugal and Coulomb barrier [9]. The lowest partial wave that can contribute is, in both cases, $\ell = 2$. Furthermore, we assume a channel radius of $a = 6.2$ fm. This radius was derived from the slope parameter, $\hbar^2/2I = 0.19$ MeV, of the rotational band to which the 2^+ state presumably belongs (cf. Sec. I), if we assume a rigid rotator composed of two pointlike particles.[2] We thus obtain

$$\frac{\gamma^2_{\alpha(\mathrm{gs})}}{\gamma^2_{\alpha(3.56)}} = \frac{P_2(0.870\ \mathrm{MeV})}{P_2(4.433\ \mathrm{MeV})} \times \frac{\Gamma_{\alpha(\mathrm{gs})}}{\Gamma_{\alpha(3.56)}} < \frac{0.051}{3.0} \times 0.04 = 0.7 \times 10^{-3}\ .$$

In the $d + {}^8$Be(gs) decay spectrum we see a fairly broad ($\Gamma \sim 0.5$ MeV) peak centered at 8.76 MeV, which we interpret as a mixture of the (3^+), $T = 0$ state at 8.68 MeV and the $2^+/3^-$ doublet. A significant background and lacking knowledge of the width of the 8.68-MeV state prevent a precise determination of the relative intensities. A rough estimate leads to $\Gamma_d/\Gamma_{\alpha(3.56)} \sim 0.5$ for the 2^+ state (if we assume that the deuteron width of the 3^- state is negligible), which corresponds to $\gamma^2_d/\gamma^2_{\alpha(3.56)} \sim 0.02$.

We note that Ref. [10] gives a combined ratio of $(\Gamma_{\alpha(\mathrm{gs})} + \Gamma_d)/\Gamma_{\alpha(3.56)} = 0.39(23)$, consistent with our results.

B. The 11.48-MeV state

The 11.48-MeV state was only seen in the $\alpha + {}^6$Li(3.56) decay spectrum. The energy of this state was determined to be 11.48(3) MeV and the width to be $\Gamma = 0.46(7)$ MeV, in reasonable agreement with the evaluated energy and width (see Table I). The energy and width were determined by fitting the peak labeled $\alpha 8$ in the hatched histogram of Fig. 4(b) with a Breit-Wigner function on top of smooth background. Different background functions (linear and quadratic) and different fit regions (narrow and wide) were used to estimate the uncertainty on the energy and width determination owing to the modeling of the background.

The 11.48-MeV state was not seen in the $\alpha + {}^6$Li(gs) decay spectrum. This allows us to place an upper limit on the ratio $\Gamma_{\alpha(\mathrm{gs})}/\Gamma_{\alpha(3.56)}$. Corrected for detection efficiencies, the upper limit is

$$\frac{\Gamma_{\alpha(\mathrm{gs})}}{\Gamma_{\alpha(3.56)}} < 0.2$$

at 95% C.L. The corresponding ratio of reduced widths is (see previous section for details)

$$\frac{\gamma^2_{\alpha(\mathrm{gs})}}{\gamma^2_{\alpha(3.56)}} = \frac{P_4(3.426\ \mathrm{MeV})}{P_4(6.989\ \mathrm{MeV})} \times \frac{\Gamma_{\alpha(\mathrm{gs})}}{\Gamma_{\alpha(3.56)}} < \frac{0.60}{2.9} \times 0.2 = 0.04.$$

We briefly comment on the limits deduced on other decay branches: Though not discussed in any detail here, we have also analyzed the final states $p + \alpha + {}^9$Be, $d + 3\alpha$, and $n + p + 3\alpha$ to look for other decay branches of the 11.48-MeV state, but we are only able to deduce rather weak upper limits, mainly due to the presence of intense competing channels which we are only able to partially subtract.[3] Examples of such competing channels are $p + {}^{13}$C leading to both $p + \alpha + {}^9$Be and $n + p + 3\alpha$, $d + {}^{12}$C leading to $d + 3\alpha$, ^{5}Li + ^{9}Be and ^{5}He + ^{9}B both leading to $n + p + 3\alpha$, and ^{6}Li + ^{8}Be leading to both $d + 3\alpha$ and $n + p + 3\alpha$. In the case of the five-body final state, $n + p + 3\alpha$, we additionally suffer from a reduced detection efficiency (by a factor of 5). The upper limits deduced at 95% C.L. are $\Gamma_x/\Gamma_{\alpha(3.56)} \lesssim 1.0$ on the decay branches leading to $p + {}^9$Be and $d + 2\alpha$ and $\Gamma_x/\Gamma_{\alpha(3.56)} \lesssim 5.0$ on the decay branches leading to $n + p + 2\alpha$.

In the recent measurement of the reaction $p + {}^9\mathrm{Be} \rightarrow \alpha + {}^6$Li(3.56) a new state was found in ^{10}B at 11.63(7) MeV with a width of $\Gamma = 0.48(15)$ MeV [10]. The spin-parity was determined to be 1^-. Given that the energy and width of this state nearly coincide with the energy and width of the 11.48-MeV state, it is tempting to conclude that they are the same state. However, according to Ref. [10] the 1^- state has

[2] For two pointlike particles of mass $4M$ and $6M$, separated by a distance a, the moment of inertia is $I = (14/5)Ma^2$.

[3] This is particularly true for channels that only involve broad intermediate states. Channels involving a narrow intermediate state are usually straightforward to identify and subtract.

$\Gamma_p/\Gamma_{\alpha(3.56)} = 20(12)$, which should have allowed us to see it clearly in the $p + {}^9$Be decay spectrum. No indication of the state was seen and, as discussed above, an upper limit of $\Gamma_p/\Gamma_{\alpha(3.56)} \lesssim 1.0$ was obtained at 95% C.L. Therefore, we conclude that the 11.48-MeV state found by us and the 1^- state found by Ref. [10] are different states.

We conjecture that the 11.48-MeV state is the analog of the 10.15-MeV, (4^+) state in ^{10}Be, which has been observed [13] to decay to the 0^+ ground state and the 2^+ first-excited state in ^{6}He with comparable intensities. We expect the 11.48-MeV state to behave similarly; i.e., in addition to the observed decay branch to the 0^+, $T = 1$ state in ^{6}Li at 3.56 MeV, there should be a decay branch to the 2^+, $T = 1$ state, which is situated at 5.37 MeV and has a rather large width of $\Gamma = 0.54$ MeV. Unfortunately, this state preferentially decays to $n + p + \alpha$ which, as discussed above, makes it very difficult to detect in the present experiment.

The 11.48-MeV state was populated too weakly to be seen in the α singles spectrum. This prevented a determination of the angular distribution of the primary α particle which could have been used to constrain the spin and parity of the state. By studying the angular correlation between the primary and the secondary α particle we were, however, able to conclude that the 11.48-MeV state must have nonzero spin. We do not attempt a quantitative analysis of the angular-correlation distribution because the quality of the experimental data is inadequate to distinguish among different spins and parities.

V. CONCLUSION

We have used the $^3\mathrm{He} + {}^{11}\mathrm{B} \rightarrow \alpha + {}^{10}\mathrm{B}$ reaction at 8.5 MeV to study the decay of states in ^{10}B. Using highly segmented detectors in a compact geometry we are able to obtain complete kinematical information for final states consisting of up to five particles. This capability allows us to clearly identify a state at 11.48(3) MeV with a width of $\Gamma = 0.46(7)$ MeV, which we identify with a state at 11.52(4) MeV in the current $A = 10$ evaluation [16]. The 11.48-MeV state is seen to decay by α emission to the 0^+, $T = 1$ state in ^{6}Li at 3.56 MeV, which leads us to identify it with a state recently observed at ~11.3 MeV, which also was seen to decay by α emission to the 3.56-MeV state [14]. We also argued why it should not be identified with a new 1^- state recently found at 11.63 MeV in a measurement of the reaction $p + {}^9\mathrm{Be} \rightarrow \alpha + {}^6\mathrm{Li}(3.56)$ [10].

We deduce an upper limit of $\Gamma_{\alpha(\mathrm{gs})}/\Gamma_{\alpha(3.56)} < 0.2$ at 95% C.L. on the decay branch to the ground state in ^{6}Li, which translates into an upper limit of $\gamma^2_{\alpha(\mathrm{gs})}/\gamma^2_{\alpha(3.56)} < 0.04$ on the reduced width. Only rather weak upper limits could be deduced on the competing decay branches: $\Gamma_x/\Gamma_{\alpha(3.56)} \lesssim 1.0$ on decay branches leading to $p + {}^9$Be and $d + 2\alpha$, and $\Gamma_x/\Gamma_{\alpha(3.56)} \lesssim 5.0$ on decay branches leading to $n + p + 2\alpha$ which includes the α-decay branch to the 2^+, $T = 1$ state in ^{6}Li at 5.37 MeV.

For the 2^+ state at 8.89 MeV we find $\Gamma_{\alpha(\mathrm{gs})}/\Gamma_{\alpha(3.56)} < 0.04$ at 95% C.L. and $\Gamma_d/\Gamma_{\alpha(3.56)} \sim 0.5$, which translates into $\gamma^2_{\alpha(\mathrm{gs})}/\gamma^2_{\alpha(3.56)} < 0.7 \times 10^{-3}$ and $\gamma^2_d/\gamma^2_{\alpha(3.56)} \sim 0.02$.

The fact that the 11.48-MeV state was not seen in the recent measurement of the reaction $p + {}^9\mathrm{Be} \rightarrow \alpha + {}^6\mathrm{Li}(3.56)$ [10] suggests that the admixture of the $p + {}^9$Be configuration in the wave function of the 11.48-MeV state is small, which is consistent with the state not decaying to $p + {}^9$Be either.

The presence of an α-decay branch to the $(T = 1)$ 3.56-MeV state in ^{6}Li combined with the absence of an α-decay branch to the $(T = 0)$ ground state in ^{6}Li strongly suggests that the 11.48-MeV state should be assigned isospin $T = 1$. The similarity between the decay characteristics of the 11.48-MeV state and the 10.15-MeV, (4^+) state in ^{10}Be leads us to conjecture that they are analog states. This would establish the 11.48-MeV state as the third member of a rotational band built on the 0^+, $T = 1$ state at 7.56 MeV, the second member of the band being the 2^+, $T = 1$ state at 8.89 MeV. A slope parameter of $\hbar^2/2I = 0.19$ MeV is deduced from the energy separation of the band members, which nearly equals the slope parameter of 0.20 MeV of the analog band in ^{10}Be. This may be compared to the ground-state bands in ^{8,9,10}Be, which have slope parameters of 0.57, 0.53, and 0.56 MeV, respectively. The small slope parameter (large moment of inertia) implies a pronounced molecular structure and a greatly enhanced separation of the two α clusters. However, experimental determination of the spin and parity of the 11.48-MeV state is needed to fully establish this picture. Improved upper limits on the competing decay branches (n, p, d) could provide complementary evidence for the asserted molecular structure.

A repetition of the present experiment would benefit from a nonplanar arrangement of the detectors, which would improve the triple-coincidence detection efficiency by an order of magnitude for the 11.48-MeV state.

ACKNOWLEDGMENTS

We acknowledge the support of the Spanish CICYT research Grant No. FPA2009-07387 and the MICINN Consolider Project No. CSD 2007-00042 as well as the support of the European Union VI Framework through RII3-EURONS/JRA4-DLEP (Contract No. 506065). OSK acknowledges support from the Villum Kann Rasmussen Foundation.

[1] L. R. Hafstad and E. Teller, Phys. Rev. **54**, 681 (1938).
[2] W. von Oertzen, M. Freer, and Y. Kanada-En'yo, Phys. Rep. **432**, 43 (2006).
[3] H. T. Fortune and R. Sherr, Phys. Rev. C **84**, 024304 (2011).
[4] N. Curtis, D. D. Caussyn, N. R. Fletcher, F. Marechal, N. Fay, and D. Robson, Phys. Rev. C **64**, 044604 (2001).
[5] N. Curtis *et al.*, Phys. Rev. C **70**, 014305 (2004).
[6] M. Milin *et al.*, Nucl. Phys. A **753**, 263 (2005).
[7] M. Freer *et al.*, Phys. Rev. Lett. **96**, 042501 (2006).
[8] J. A. Liendo, N. Curtis, D. D. Caussyn, N. R. Fletcher, and T. Kurtukian-Nieto, Phys. Rev. C **65**, 034317 (2002).
[9] A. M. Lane and R. G. Thomas, Rev. Mod. Phys. **30**, 257 (1958).

[10] A. N. Kuchera *et al*., Phys. Rev. C **84**, 054615 (2011).
[11] M. Milin, Int. J. Mod. Phys. E **20**, 759 (2011).
[12] N. Soic *et al*., Europhys. Lett. **34**, 7 (1996).
[13] D. Miljanić *et al*., FIZIKA B (Zagreb) **10**, 235 (2001).
[14] M. Uroić *et al*., AIP Conf. Proc. **1165**, 31 (2009).
[15] D. R. Tilley *et al*., Nucl. Phys. A **708**, 3 (2002).
[16] D. R. Tilley *et al*., Nucl. Phys. A **745**, 155 (2004).
[17] M. Alcorta *et al*., Nucl. Instrum. Methods Phys. Res., Sect. A **605**, 318 (2009).
[18] O. S. Kirsebom, Ph.D. thesis, Aarhus University, 2010.
[19] O. S. Kirsebom *et al*., Phys. Lett. B **680**, 44 (2009).
[20] J. D. Purvis, F. Ajzenberg-Selove, and L. M. Polsky, Phys. Rev. **162**, 1005 (1967).
[21] O. S. Kirsebom *et al*., Phys. Rev. C **81**, 064313 (2010).